

Summary of chemotaxis in porous media

Elliot Marsden

July 2014

Contents

1	Diffusion of active particles in a continuous environment	2
2	Drift of chemotactic active particles in a continuous environment	2
3	Diffusion of active particles in a porous environment	4
4	Drift of chemotactic active particles in a porous environment	6
	Appendix A: Normalisation of temporal chemotaxis integral	6
	Appendix B: Derivation of expression for drift speed of ABPs doing spatial chemotaxis	8

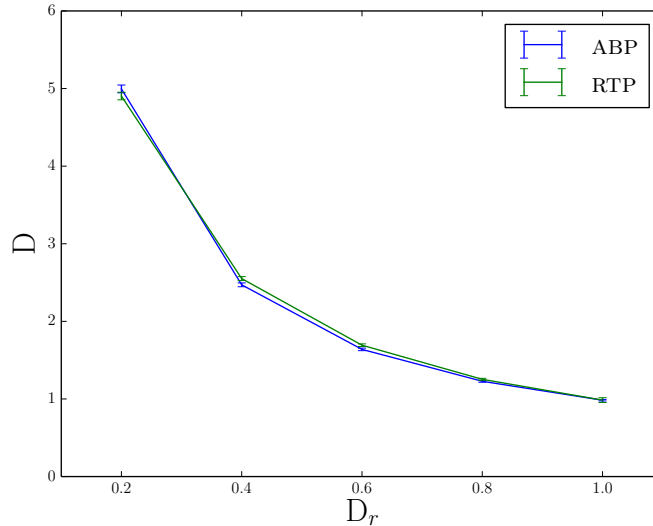


Figure 1: Diffusivity of active particles in free space as a function of the effective rotational diffusion constant. For RTPs, α is equivalent to D_r over long time intervals.

1 Diffusion of active particles in a continuous environment

We investigate two types of active particle: Active Brownian Particles (ABPs), whose direction diffuses slowly with rotational diffusion constant D_r , and Run and Tumble Particles (RTPs), whose direction is completely randomised at a uniform rate α . Over long time intervals, the free-space diffusivity of the two particles is the same (Fig. 1).

2 Drift of chemotactic active particles in a continuous environment

We allow for chemotaxis in the dynamics of both particle types by first introducing a measure, the ‘chemotactic fitness’ of a particle trajectory, $f(\mathbf{v}(t), c(t))$, where $c(t)$ is the chemical concentration at the particle’s position at time t .

Secondly, we vary the strength of the particle’s rotational noise according to f : for ABPs, $D_r = D_r(f)$ (for RTPs replace D_r with the tumbling rate α).

We choose a linear response for D_r :

$$D_r(f) = D_{r,0}(1 - f) \quad (1)$$

where $D_{r,0}$ is the free-space rotational diffusion constant.

We investigate two forms for f . The first is proportional to the instantaneous degree of alignment between the particle's direction and the chemical gradient,

$$\begin{aligned} f_s &= \chi \frac{\dot{c}}{v}, \\ \dot{c} &= \mathbf{v}(t) \cdot \nabla c(t), \end{aligned} \quad (2)$$

where χ controls the strength of the chemotactic response. \dot{c} represents the time-derivative of the chemical concentration in the particle's reference frame. The second form is a time-averaged approximation of the first:

$$\begin{aligned} f_t &= \chi \frac{\tilde{c}}{v}, \\ \tilde{c} &= N \int_0^t K(t - t') c(t') dt', \end{aligned} \quad (3)$$

where K is a kernel which acts to transform the particle's measured chemical concentration history into an approximate co-moving chemical concentration change, and N is a normalisation constant. N is chosen such that a particle moving directly up a constant chemical gradient with no rotational noise, gives the same value for f_s and f_t (see Appendix A).

We refer to particles using f_s as doing 'spatial chemotaxis', and those using f_t as doing 'temporal chemotaxis'.

We investigate the behaviour of these particle in an environment with a chemical gradient that is constant in time and space, of magnitude 1 in the direction $\hat{\mathbf{u}}_c$. The effectiveness of chemotaxis is measured by the drift speed in the direction of the gradient, $v_d = \langle \mathbf{v} \cdot \nabla c \rangle$. Figure 2 shows the effect of changing the strength of chemotaxis on the drift speed, alongside a comparison with theoretical predictions for ABPs (see Appendix B). For spatial chemotaxis, ABPs and RTPs have identical drift speeds. For temporal chemotaxis, this equivalence breaks down: RTPs do temporal chemotaxis more effectively than ABPs.

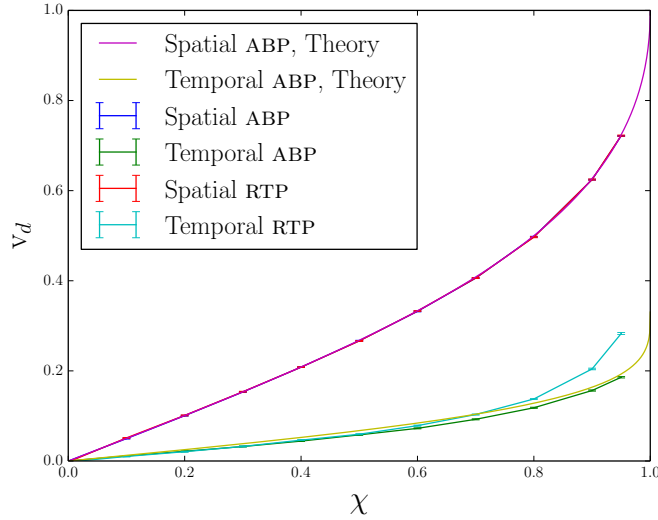


Figure 2: The dependence of the drift speed of ABPs and RTPs in free space, on the chemotaxis strength parameter, χ , for ‘spatial’ and ‘temporal’ chemotaxis. The two ‘spatial’ curves lie on top of one another. Also shown are theoretical predictions for both ABP curves.

3 Diffusion of active particles in a porous environment

We now look at the behaviour of non-chemotactic active particles in porous environments formed by randomly placed non-overlapping circles of a constant radius, up to some packing fraction, ϕ . A particle colliding with such an obstacle reverses its velocity component perpendicular to the obstacle surface (that is, it bounces off the obstacle).

Figure 3 shows the effect of obstructing ABPs on how fast they diffuse through the environment. As expected, higher packing fractions cause the particles to diffuse more slowly. In free space, reducing the amount of rotational noise always increases the diffusivity, however in a porous medium this is no longer strictly true, as can be seen in Fig. 4. A very low amount of rotational noise means the particles collide with the environment frequently, so some noise is useful in helping the particles navigate through the environment.

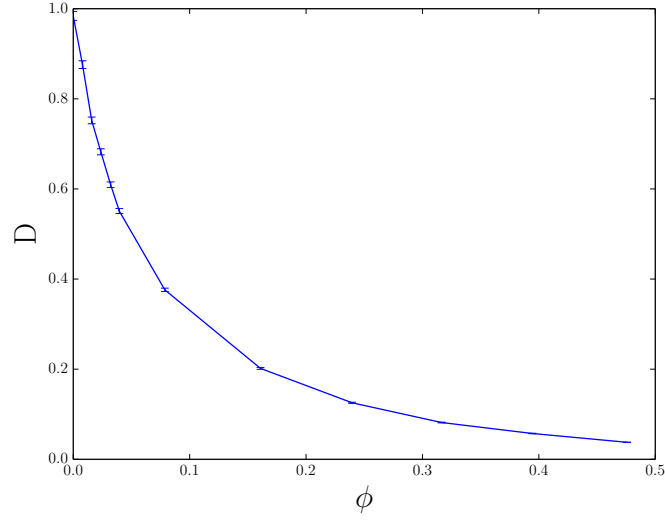


Figure 3: The diffusivity of ABPs in a porous medium as a function of the packing fraction.

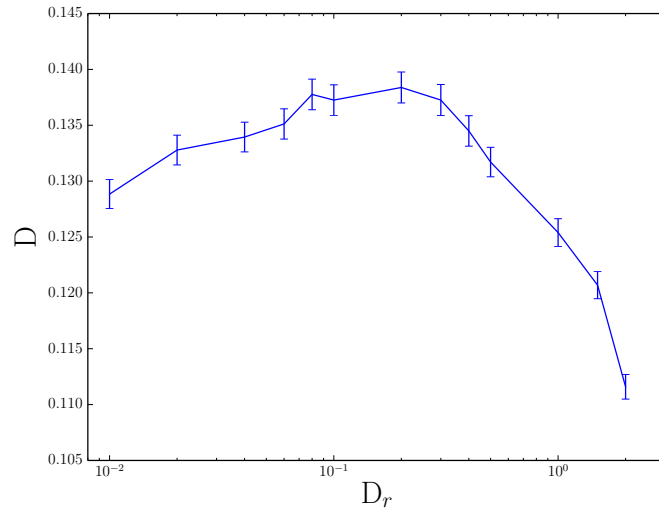


Figure 4: The dependence of the diffusivity of ABPs in a porous medium, with constant packing fraction $\phi = 24\%$, on the rotational diffusion constant.

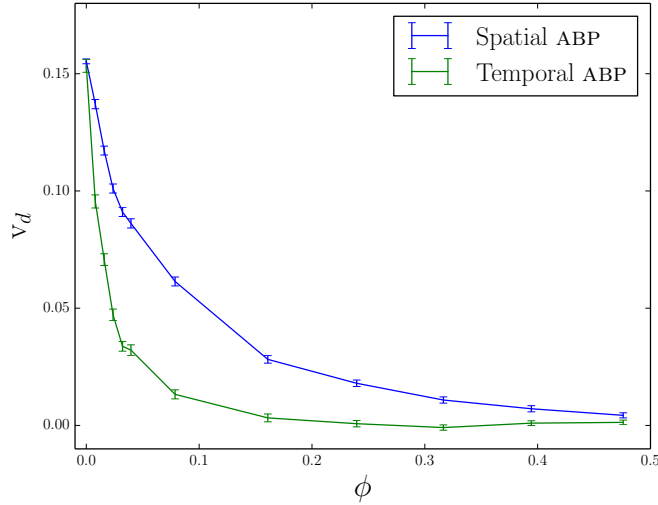


Figure 5: The dependence of the drift speed of ABPs in a porous medium, on the packing fraction, for ‘spatial’ and ‘temporal’ chemotaxis. For spatial chemotaxis, $\chi = 0.304$ was used, and for temporal $\chi = 0.9$; chosen such that the free-space drift speeds are identical.

4 Drift of chemotactic active particles in a porous environment

For ‘spatial’ and ‘temporal’ chemotaxis with ABPs, we choose χ for both such that the free-space drift speeds are identical, and investigate how effective chemotaxis is as the packing fraction changes. Figure 5 shows that particles doing spatial chemotaxis are more effective than those doing temporal chemotaxis in the same environment. This is presumably due to collisions with obstacles disrupting the time averaging being done in the latter case.

Appendix A: Normalisation of temporal chemotaxis integral

Maximum fitness of spatial chemotaxis

Assume a chemical gradient constant in time and space, of magnitude 1, in direction $\hat{\mathbf{u}}_c$. From Eq. (2),

Parameter	Label	Value
Dimension	d	2
System size	L	1
Time-step	dt	0.001
Number of particles	n	10^4
Particle speed	v	1
Base rotational diffusion constant	$D_{r,0}$	1
Base tumble rate	α_0	1
Obstacle radius	R	0.05

Table 1: Parameters used in all simulations, except where indicated otherwise.

$$\begin{aligned}
f_s &= \chi \frac{\dot{c}}{v}, \\
\dot{c} &= \mathbf{v}(t) \cdot \hat{\mathbf{u}}_c \\
&= v \cos \theta.
\end{aligned} \tag{4}$$

Clearly then the maximum fitness is when $\theta = 0$, that is, when the particle moves directly up the concentration gradient. In this case, $\dot{c} = v$, and $f_s = \chi$.

Calibrating temporal chemotaxis

We want the maximum fitness to be the same for spatial and temporal chemotaxis. From Eq. (3) we can see that this requires $f_{t,\max} = \chi$, and thus $\tilde{c}_{\max} = v$.

We assume that the fitness is again maximised when the particle moves directly up the chemical gradient, $\mathbf{v} = v\hat{\mathbf{u}}_c$. This means that the chemical concentration at the particle's position at time t is,

$$\begin{aligned}
c(t) &= c(0) + (\mathbf{v} \cdot \hat{\mathbf{u}}_c)t \\
&= c(0) + vt.
\end{aligned} \tag{5}$$

Substituting Eq. (5) into Eq. (3),

$$\begin{aligned}
\tilde{c} &= N \int_0^t K(t-t') (c(0) + vt') dt' \\
&= N \left(c(0) \int_0^t K(t-t') dt' + v \int_0^t K(t-t') t' dt' \right).
\end{aligned} \tag{6}$$

The particular form we use for K is

$$K(t) = \exp(-t) \left(1 - \frac{t}{2} - \frac{t^2}{4} \right) \quad (7)$$

Assuming the particle points up the chemical gradient for a sufficiently long time, we can take $t \rightarrow \infty$. Computing the first integral in this limit gives

$$\begin{aligned} \int_0^\infty K(-t) dt &= \left[\frac{1}{4} \exp(-t) t (t + 4) \right]_0^\infty \\ &= 0. \end{aligned} \quad (8)$$

This means that the first term in Eq. (6) vanishes. Computing the second integral in the same limit,

$$\begin{aligned} \int_0^\infty t K(-t) dt &= \left[\frac{1}{4} \exp(-t) (t(t+2)(t+3) + 6) \right]_0^\infty \\ &= \frac{3}{2}. \end{aligned} \quad (9)$$

So using Eqs. (8) and (9) in Eq. (6),

$$\tilde{c} = \frac{3}{2} N v. \quad (10)$$

This means that for our spatial and temporal chemotaxis forms to be comparable, $N = \frac{2}{3}$.

Appendix B: Derivation of expression for drift speed of ABPs doing spatial chemotaxis

Assume an environment with a chemical gradient that is constant in time and space, of magnitude 1 in the direction $\hat{\mathbf{u}}_c$. Take θ to be the angle between this and the particle's velocity. A particle swimming with orientation θ has a drift speed $v_d = v \cos \theta$. Over long times, assuming the particle ergodically samples all θ (meaning that $D_r > 0$ at all times), then the particle has an average drift speed,

$$\begin{aligned} v_d &= \int_{-\pi}^{\pi} P(\theta) v_d(\theta) d\theta \\ &= v \int_{-\pi}^{\pi} P(\theta) \cos \theta d\theta, \end{aligned} \quad (11)$$

where $P(\theta)$ is the probability of the particle being at orientation θ .

From simulations, for spatial chemotaxis we find that $P(\theta) \propto \frac{1}{D_r(\theta)}$. This means that,

$$P(\theta) = \frac{D_r(\theta)^{-1}}{\int_{-\pi}^{\pi} D_r(\theta)^{-1} d\theta}. \quad (12)$$

Calculating the normalisation constant

Substituting Eq. (2) into Eq. (1),

$$\begin{aligned} D_r(\theta) &= D_{r,0} (1 - f_s) \\ &= D_{r,0} \left(1 - \chi \frac{\dot{c}}{v} \right) \\ &= D_{r,0} \left(1 - \chi \frac{\mathbf{v}(t) \cdot \hat{\mathbf{u}}_c}{v} \right) \\ &= D_{r,0} (1 - \chi \cos \theta) \end{aligned} \quad (13)$$

$$\begin{aligned} I &:= \int_{-\pi}^{\pi} D_r(\theta)^{-1} d\theta \\ &= \frac{1}{D_{r,0}} \int_{-\pi}^{\pi} \frac{d\theta}{1 - \chi \cos \theta} \\ &= -\frac{1}{D_{r,0}} \left[\frac{2}{\sqrt{\chi^2 - 1}} \tanh^{-1} \left(\frac{(\chi + 1) \tan \left(\frac{\theta}{2} \right)}{\sqrt{\chi^2 - 1}} \right) \right]_{-\pi}^{\pi} \end{aligned} \quad (14)$$

Using the fact that \tanh^{-1} and \tan are odd functions,

$$I = -\frac{1}{D_{r,0}} \frac{4}{\sqrt{\chi^2 - 1}} \tanh^{-1} \left(\frac{(\chi + 1) \tan \left(\frac{\pi}{2} \right)}{\sqrt{\chi^2 - 1}} \right). \quad (15)$$

Given that $\tan \left(\frac{\pi}{2} \right) = \infty$, and $\tanh^{-1}(\infty) = -\frac{i\pi}{2}$, then

$$I = \frac{1}{D_{r,0}} \frac{2\pi i}{\sqrt{\chi^2 - 1}}. \quad (16)$$

We know that $\chi < 1$ as this is required for $D_r > 0 \forall \theta$, so we can factor out i , finally giving the normalisation constant as

$$I = \frac{1}{D_{r,0}} \frac{2\pi}{\sqrt{1-\chi^2}}. \quad (17)$$

Deriving an expression for the drift speed

We can now calculate the actual drift speed by substituting: Eq. (17) into Eq. (11):

$$\begin{aligned} v_d &= v \int_{-\pi}^{\pi} P(\theta) \cos \theta \, d\theta \\ &= v \frac{\sqrt{1-\chi^2}}{2\pi D_{r,0}} \int_{-\pi}^{\pi} \frac{\cos \theta}{1-\chi \cos \theta} \, d\theta. \end{aligned} \quad (18)$$

Integrating this and simplifying through almost identical steps as for the normalisation constant gives,

$$v_d = v \frac{1 - \sqrt{1-\chi^2}}{\chi}. \quad (19)$$